Double-slit experiment revisited

Siddhant Das[*], Dirk-André Deckert[*], Leopold Kellers[*], Simon Krekels[†,‡], and Ward Struyve[†,$]

[*]Mathematisches Institut, Ludwig-Maximilians-Universität München
[†]Department of Physics and Astronomy, KU Leuven
[‡]Imec, Leuven
[$]Centre for Logic and Philosophy of Science, KU Leuven

May 20, 2025

Abstract

The double-slit experiment is one of the quintessential quantum experiments. However, it tends to be overlooked that the build-up of the interference pattern involves single detection events with a random position and a random time of detection. Hence, a full theoretical account of this experiment requires the specification of the joint position and time distribution of detection at the screen, whose position marginal yields the famous interference pattern. The difficulty lies in what this distribution should be. While there are a variety of proposals for a quantum mechanical time observable, there is no consensus about the right choice. Here, we consider Bohmian mechanics, which allows for a natural and practical approach to this problem. We simulate this distribution in the case of an initial Gaussian wave packet passing through a double-slit potential. We also consider a more challenging setup in which one of the slits is closed during flight. To experimentally probe the quantum nature of the time distribution, a sufficient longitudinal spread of the initial wave packet is required, which has not been achieved so far. Without sufficient spread, the temporal aspect of the distribution can be treated classically. We illustrate this for the case of the double-slit experiment with helium atoms by Kurtsiefer *et al.* Nature **386**, 150 (1997), which reports the joint position and time distribution.

1 Introduction

Diffraction and interference phenomena occupy a prominent place in the phenomenology of quantum physics, Young's double-slit experiment (DSE) being an archetypal example which according to Feynman "has in it the heart of quantum mechanics" [1]. Quantum physicists have discussed the DSE and augments thereof, e.g., the which-way [2, 3], or the delayed-choice DSE [4], with varying degrees of rigour. Several notable realizations employing *single* electrons [5, 6], neutrons [7, 8], atoms [9, 10], and even macro-molecules [11] have been performed.

The interference fringes in a DSE are formed by the accumulation of single-particle impact positions on a screen. What tends to be overlooked, however, is that each imprinted position with screen coordinates (x, y) is associated with a definite, but random, time of flight[1] (ToF) t_f, given by the (measured) time of detection on the screen minus the (known) time of emission at the source. Therefore, specifying the joint distribution $\rho(x, y, t_f)$—whose marginal $\int \mathrm{d}t_f\, \rho(x, y, t_f)$ provides

[1]Also known as arrival time, transit time, or detection time.

the pattern of the fringes—is indispensable for a full account of the DSE, or any other scattering experiment for that matter[12–15].

One might be inclined to think that the distribution $\rho(x, y, t_f)$ on the screen corresponds to $|\psi(x, y, d, t_f)|^2$, where $\psi(x, y, z, t)$ is the particle's wave function at time t and $z = d$ the detection plane. But this is incorrect because $|\psi(x, y, z, t)|^2$ is, according to Born's rule, the distribution of *positions* detected at a *specified time* t, while what is needed is a joint distribution of *positions* and *times* detected at a *specified surface*.[2]

Nevertheless, under certain conditions, such as a narrow spread in the longitudinal direction, i.e., in the direction towards the screen, which tend to apply to present-day experiments, the detection times at the screen can be treated classically, leading in effect to a joint distribution that is well approximated by $|\psi|^2$ [14, Eq. (9)]. This is something that needs to be taken into account in order to really probe the quantum nature of the time distribution.

While there is no recognized observable for time in quantum mechanics, in contrast to position, there is a multitude of (disparate) ToF proposals [16–18] (some of them being questionable [19–25]). Barring a few works checking tunneling-time predictions, e.g., [26–30], surprisingly, so far none of the ToF proposals have been benchmarked against experiment.

The goal of this paper is to consider the Bohmian approach to this problem, by considering the first-passage (or hitting) distribution, i.e., the joint distribution of times and locations of particles crossing the detection screen. While this approach ignores the possible effect of the screen itself, this seems a natural and practicable approximation. The potential for treating ToF experiments this way has long been recognized [13, 31–34], with numerous applications to arrival- and tunneling-time problems [35–52]. In section 2, we will consider the DSE setup and simulate the evolution of an initial Gaussian wave packet passing through the slits. The first-passage distribution of the Bohmian trajectories is considered for three different placements of the detection screen, leading to qualitatively different behavior. Subsequently, we consider a challenging variant of the DSE, dubbed the dynamic DSE, in which one of the slits is closed during flight. This serves as an illustration of the potency of the adopted approach.

On the experimental side, Kurtsiefer, Pfau, and Mlynek (hereafter KPM) [10, 53, 54] reported the joint position-time distribution using metastable (i.e., electronically excited) helium atoms (see below for further details). In [53], two marginal distributions are plotted: Fig. 1a shows the distribution of (x, y) on the screen, while Fig. 1b shows that of (x, t_f). In [10], the joint distribution is plotted for three different distances of the detection screen, see Fig. 6. The Bohmian first-passage distribution, shown in 3a, shows striking similarity. However, this similarity is deceptive, as these plots concern different quantum ensembles. As we will explain in section 3, in our Bohmian analysis we assumed an ensemble where each wave function is the same and has an appreciable longitudinal spread. The ensemble considered by KPM, on the other hand, concerns a mixture of wave functions whose longitudinal velocity is thermally distributed, and which do not have appreciable longitudinal spread. So in the latter case the temporal spread is not due to the longitudinal spread of the wave function, but due to the random initial longitudinal velocity, allowing KPM to treat the ToF classically. This also seems to be the case in other interference experiments to date. To actually probe the quantum nature of the time distribution, it is important to consider similar experimental setups for which the longitudinal spread of each initial wave function in the mixture has a considerable contribution to the temporal spread of the joint distribution.

[2]The conjectured quantity is not even normalizable in simple examples. Therefore, it cannot be a legitimate probability density.

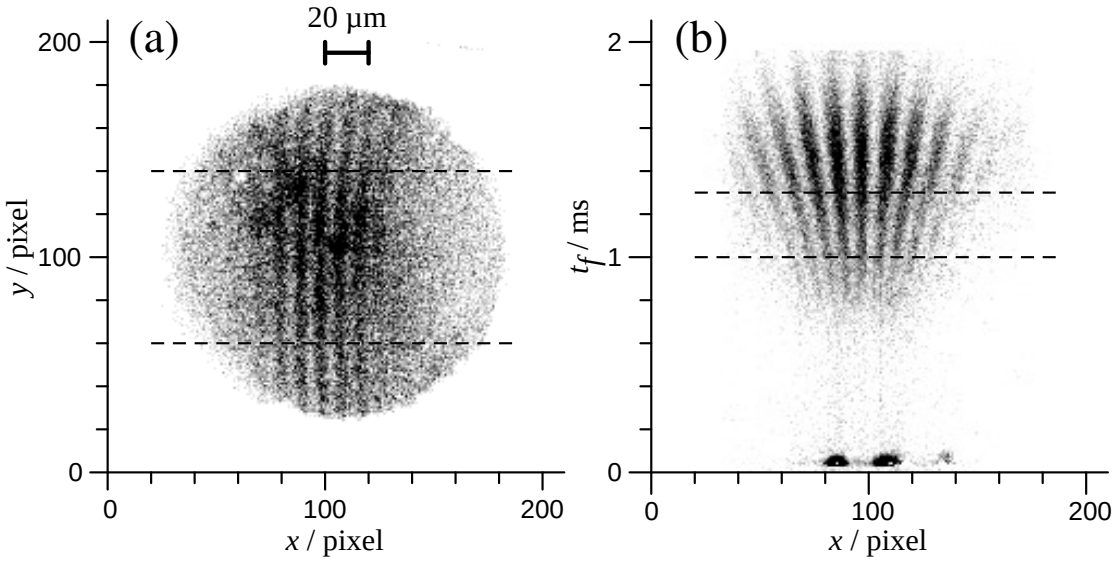

Figure 1: Figures from the KPM experiment [53] (reproduced with permission). **(a)** Double-slit interference pattern observed on a screen after many single-atom detection events. **(b)** Joint distribution of the ToF t_f and the x-screen-coordinate of the detection events. Impact positions of atoms arriving in the t_f range indicated by the dashed lines in (b) were accumulated to produce (a). A fraction of very fast atoms emanating from the source cast a shadow of the slits at the bottom.

2 Bohmian account of the DSE

2.1 Trajectories for the DSE

Bohmian mechanics (also called the de Broglie-Bohm theory or pilot-wave theory) is a theory describing point particles moving along trajectories that grounds the formalism and predictions of standard quantum mechanics [15, 55–57]. For a single-particle with position $\mathbf{R}$ and mass m, the dynamics is given by the guidance equation

$$\dot{\mathbf{R}}(t) = \frac{\hbar}{m}\,\mathrm{Im}\left[\frac{\boldsymbol{\nabla}\psi\big(\mathbf{R}(t),t\big)}{\psi\big(\mathbf{R}(t),t\big)}\right], \tag{1}$$

where $\psi(\mathbf{r},t)$ is the wave function satisfying Schrödinger's equation with an external potential $V(\mathbf{r},t)$. Here, the "wave/particle duality" of quantum mechanics is resolved in a trivial way: both a wave *and* a particle are present.

The motion of the particle is deterministic, i.e., given its initial position $\mathbf{R}(0)$ and wave function $\psi(\mathbf{r},0)$, it has a unique trajectory $\mathbf{R}(t)$. However, considering different experimental runs, the initial positions are random, with distribution given by $|\psi(\mathbf{r},0)|^2$—the quantum equilibrium distribution—(which implies that the position is distributed according to $|\psi(\mathbf{r},t)|^2$ at time t). As such, both the detection locations and times of a particle are random in different runs of a scattering experiment.

Bohmian trajectories for the DSE are shown in Fig. 2b, and are well-known; they feature invariably in expositions of Bohmian mechanics. DSE trajectories were first presented by Philippidis *et al.* in the late 1970s [58] and have been reproduced various times using different methods [59–62]. Most presentations make do with a freely propagating wave function, not employing a double-slit potential. Here, they are produced without this simplifying assumption. See also [63] for a weak measurement of average trajectories in a DSE, bearing resemblance to the trajectories of Fig. 2b.

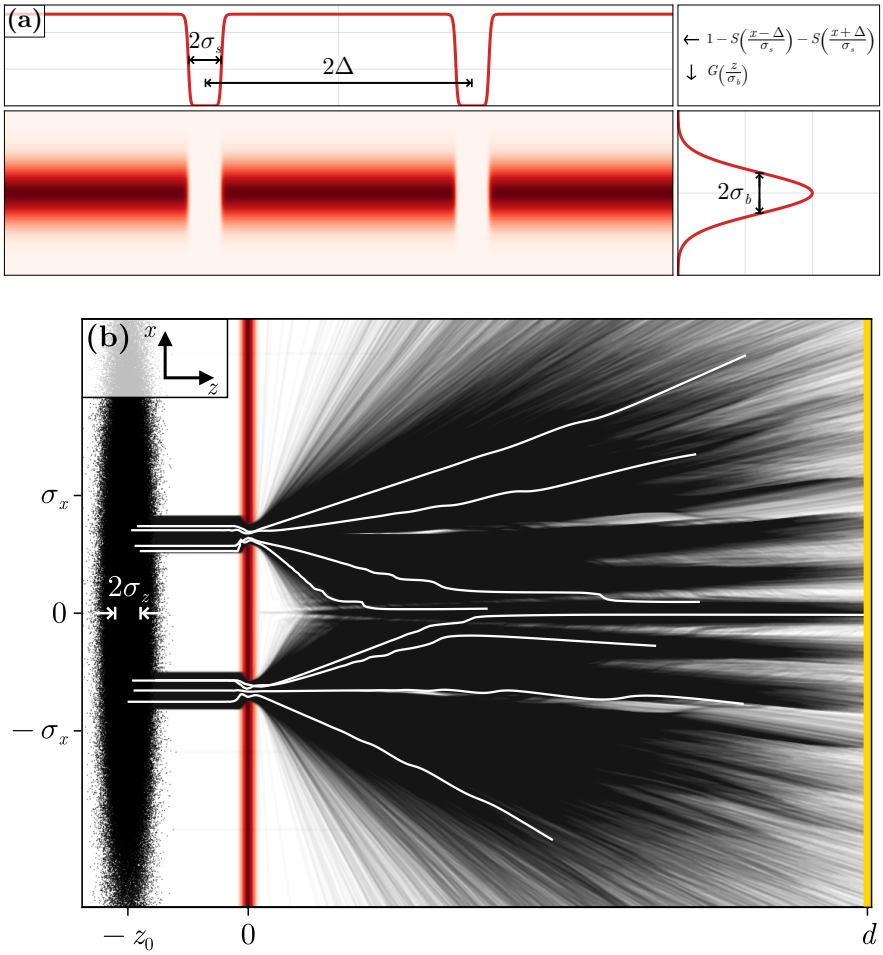

Figure 2: **(a)** Schematic illustration of the double-slit potential (3) for $f_1 = f_2 = 1$. **(b)** A collection of 5×10^5 Bohmian trajectories in the xz-plane for the DSE with initial conditions (black dots) sampled randomly from the $|\psi(\mathbf{r}, 0)|^2$-distribution. Only the trajectories which pass through the slits (i.e., those which are not back-scattered by the double-slit potential) are shown. Each curve tracks a particle that eventually strikes the detection plane $z = d$. The following potential barrier and wave packet parameters were assumed: $V_0 = 10^3$, $\sigma_b = 0.125$, $\sigma_s = 0.25$, $k_x = x_0 = 0$, $k_z = 15$, $z_0 = 2$, and $\sigma_x = 3$, $\sigma_z = 0.25$ in units where $\hbar = m = \Delta = 1$. A number of selected trajectories (in white) display the characteristic non-Newtonian meandering of the trajectories.

The trajectories provide an almost self-explanatory account of how the interference pattern builds up on a distant screen one particle at a time. In particular, they show "how the motion of a particle, passing through just one of two holes in [a] screen, could be influenced by waves propagating through both holes. And, so influenced that the particle does not go where the waves cancel out, but is attracted to where they cooperate" [64, p. 191]. It follows that interference experiments can be accounted for in terms of particle trajectories, claims to the contrary notwithstanding.[3]

To produce the Bohmian trajectories in Fig. 2b, Schrödinger's equation was solved numerically

[3]For instance, "it is clear that [the DSE] can in no way be reconciled with the idea that electrons move in paths. ... In quantum mechanics there is no such concept as the path of a particle." [65, p. 2], or that "many ideas have been concocted to try to explain the curve for P_{12} [the interference pattern] in terms of individual electrons going around in complicated ways through the holes. None of them has succeeded." [1, Sec. 1.5].

with initial Gaussian wave function centered at $(-x_0, 0, -z_0)$ in front of the slits:

$$\psi(\mathbf{r}, 0) = \frac{e^{i(k_x x + k_z z)}}{\sqrt{\sigma_x \sigma_y \sigma_z}} G\left(\frac{x + x_0}{\sigma_x}\right) G\left(\frac{y}{\sigma_y}\right) G\left(\frac{z + z_0}{\sigma_z}\right), \tag{2}$$

where $G(\xi) = \pi^{-1/4} \exp(-\xi^2/2)$.

The screen containing the slits was modeled by the Gaussian potential barrier

$$V = V_0 G\left(\frac{z}{\sigma_b}\right)\left[1 - f_1 S\left(\frac{x - \Delta}{\sigma_s}\right) - f_2 S\left(\frac{x + \Delta}{\sigma_s}\right)\right], \tag{3}$$

featuring two apertures for $f_1 = f_2 = 1$,[4] as shown in Fig. 2a. Here, $S(\xi) = 1/(1 + \xi^{16})$, 2Δ, σ_s, and σ_b respectively denote the aperture function, slit separation, slit width, and the thickness of the barrier. Throughout the present work, masses, lengths and times are expressed in units of m, Δ and $m\Delta^2/\hbar$, respectively. (This is equivalent to setting $\hbar = m = \Delta = 1$.) The Bohmian trajectories were computed by numerically integrating the guidance equation (1) for 5×10^5 initial positions randomly sampled from the $|\psi(\mathbf{r}, 0)|^2$-distribution. About 15% of the sampled trajectories made it through the slits giving rise to detection events. The rest (not shown in Fig. 2b) were back-scattered from the potential barrier.

2.2 First-passage distribution

The preceding discussion suggests that it is natural to take, as an approximation to the ToF on a specified surface $\mathcal{D}$ (such as the plane $z = d$), the first-passage time (FPT) of a Bohmian trajectory[5]:

$$t_f(\mathbf{r}_0) = \inf\left\{ t : \mathbf{R}(t) \in \mathcal{D} \text{ and } \mathbf{R}(0) = \mathbf{r}_0 \right\}, \tag{4}$$

$\mathbf{R}(t_f)$ being the concomitant crossing position on $\mathcal{D}$,[6] as a function of the random initial condition $\mathbf{r}_0$—quantities that have no respective counterparts in standard quantum theory.

Barring special circumstances, the distribution of this crossing event $(\mathbf{R}(t_f), t_f)$ is only numerically accessible. When there is no backflow (i.e., when trajectories only cross the surface $\mathcal{D}$ once), like in the cases considered here, and more generally in the far-field or scattering regime, the distribution reduces to $j_\perp(\mathbf{r}, t_f)$ [13, 66, 67], [23, p. 7]—the component of the quantum flux (or probability current) density orthogonal to the surface $\mathcal{D}$.[7]

Note that the FPT does not take into account the details of the detection. This is justified if individual detection events are triggered close to the location and time impact of Bohmian trajectories, and if the detection events do not significantly disturb the trajectories. In the present case, these assumptions seem very natural, especially in the far-field regime.

However, to be clear, it is also the case that these assumptions cannot hold in general [13–15, 68, 69].[8] First, according to Bohmian mechanics (as well as quantum mechanics), the ToF distribution must be given by a POVM [71, pp. 186-187], whereas the FPT distribution generically is not a POVM, not even in the case it is given by the flux $j_\perp(\mathbf{r}, t_f)$ [68]. Second, there are also other Bohmian-type theories, which concern different guidance equations, but which are nevertheless empirically equivalent, like Nelson's stochastic mechanics [72] and the zig-zag dynamics [73, 74]. Clearly, such theories will disagree on the FPT (see e.g., [75] and [76] for the FPT distribution in

[4] For the dynamic DSE problem considered below, $f_{1,2}$ are varied in time as per Eq. (5).

[5] One considers the FPT because in general a trajectory might cross the surface $\mathcal{D}$ more than once [40, 41]. However, this does not happen in the present setting.

[6] The infimum in (4) ensures that the FPT of trajectories not intercepting $\mathcal{D}$, e.g., those back-scattered at the plane containing the slits giving rise to non-detection events, is infinity, since $\inf \emptyset := \infty$.

[7] In one-dimensional settings there is an explicit formula [66, Eq. (12)] for the distribution of t_f defined in Eq. (4).

[8] One of us, Siddhant Das, does not agree with the statements expressed in this paragraph, see [70].

the case of the double-slit experiment). Nevertheless, because of their empirical equivalence, they will agree on the ToF. As such, ToF experiments like the one considered here cannot be used to distinguish such versions of quantum mechanics, contrary to what is sometimes claimed, see for instance [77]. They can merely benchmark the different approaches to model the ToF distribution.

A rigorous justification of the FPT as an approximation to the ToF would require actually modeling the detector, but this is easier said than done. In any case, it seems pressing to explore the ToF distribution also experimentally. In setups as considered here, an analysis of the FPT can provide valuable pointers for such endeavours.

2.3 Numerical DSE

To simulate the first-passage distribution for the DSE, Schrödinger's equation with the double-slit potential (3) was numerically solved for an initial Gaussian wave packet (2). The wave function then determines the particle velocity in the guidance equation (1).

Since the wave function evolution is simulated on a grid with Dirichlet boundary conditions, we need to avoid effects arising from reflection at the boundary, in particular reflection from the back wall. To achieve this, the slits were closed dynamically after the passage of the bulk of the wave packet, by changing the $f_{1,2}$ in (3) to

$$f = \frac{1}{2}\Big(1 + \tanh\big[\gamma\,(t_c - t)\big]\Big). \tag{5}$$

This closing of the slits of course also cuts off the back tails of the wave packet, but without significant changes to the FPT distribution of the particles passing through the slits.

Numerically integrating the guidance equation Eq. (1) for 5×10^5 initial conditions randomly sampled from the $|\psi(\mathbf{r}, 0)|^2$ distribution, the crossing position $\big(X(t_f), Y(t_f)\big)$ and time t_f of Bohmian trajectories through $z = d$ were recorded.[9] Histograms of obtained t_f and $X(t_f)$ are presented in Fig. 3a, and current densities $j_\perp(\mathbf{r}, t_f)$ at the screens are shown in Fig. 3b. The evolution of the density $|\psi|^2$ is shown in Fig. 4. The code used for the numerics is publicly available [78].

2.4 Dynamic DSE

The Bohmian method is also suitable for other setups of this type. To demonstrate this, we consider a more complex time-dependent setup, where one of the slits is closed in flight. For this, we modify only f_2 in (3), which causes the slit centered at $x = -\Delta$ to gradually close in time[10], keeping $f_1 = 1$. Scatter plots of $\big(X(t_f), t_f\big)$ for this dynamic DSE are plotted in Fig. 5 for two values of γ; a large γ implies a fast closing of the slit. The closing time t_c is chosen close to the time at which the peak of the wave packet crosses $z = 0$, i.e., z_0/k_z. Evidently, more trajectories pass through the open slit. Furthermore, the interference fringes become less pronounced for $t_f \gg t_c$, as expected for single-slit diffraction.

Note that the closing of the slits sends a shock wave through the wave packet, resulting in the banded arrivals at $t \approx 0.6$, visible in both (a) and (b). In addition, the arrivals from the closing slit end earlier in the case of slow closing rather than fast closing. This is because for small γ, while the closing of the slit goes slower, it also starts to close earlier.

[9] Since the wave function remains a separable function of (x, z) and y, the particle motion in the y-direction is independent of the motion in the (x, z)-plane and hence does not affect the FPT t_f nor the x-screen-coordinate $X(t_f)$.

[10] A dynamically controlled DSE seems well-amenable to present-day technology [5].

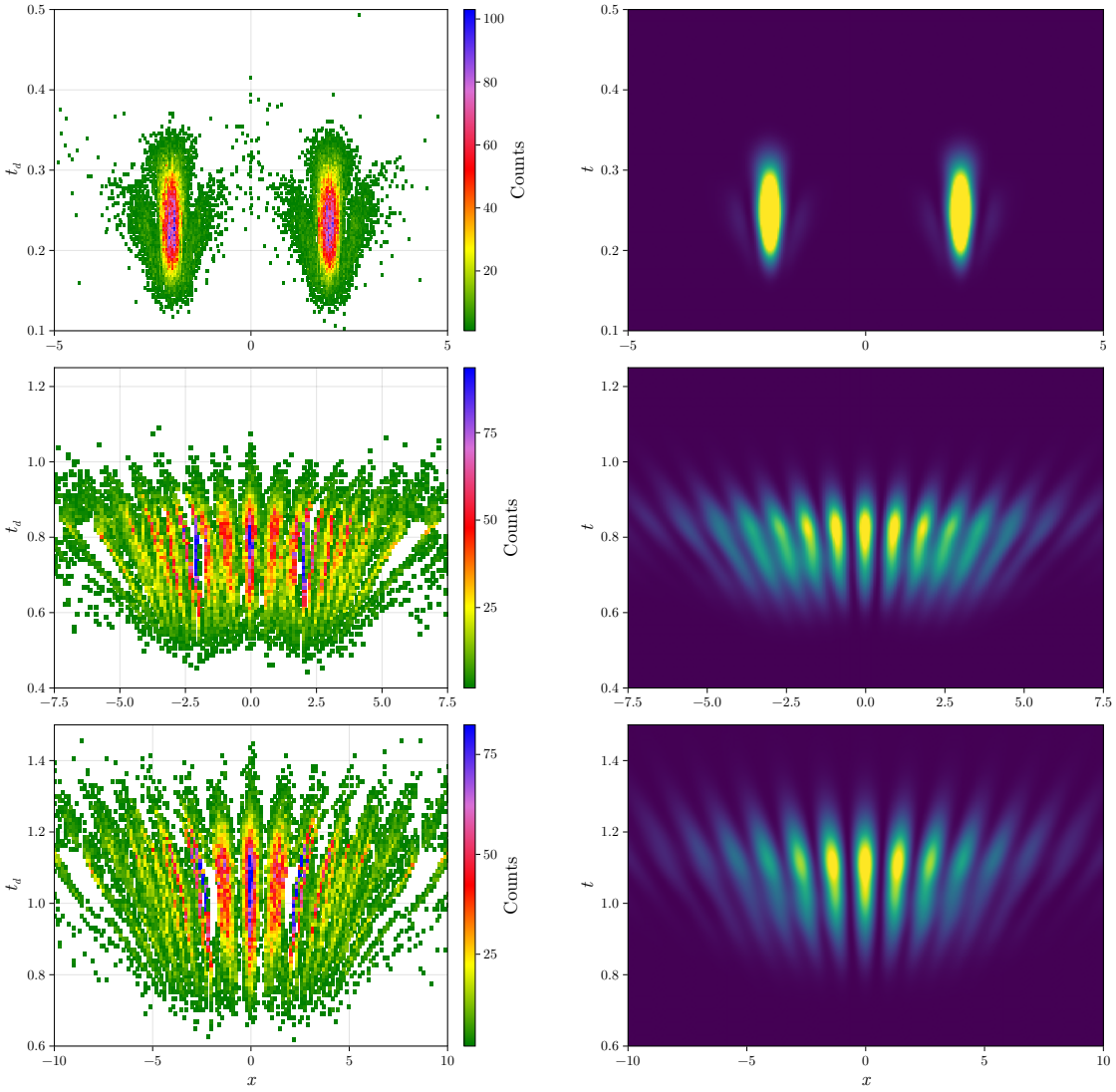

(a) Joint distributions of ToFs and x-screen coordinates for different slit-screen separations, generated from Bohmian trajectory impacts.

(b) The flux density across the screen.

Figure 3: Numerical data generated for $V_0 = 10^3$, $\sigma_b = 0.125$, $\sigma_s = 0.5$, $k_x = 0$, $k_z = 15$, $z_0 = 3$, $\sigma_x = 3$, $\sigma_z = 0.25$, with $d = 0.9$ (top), $d = 10$ (middle), and $d = 15$ (bottom), taking $\hbar = m = \Delta = 1$. (The slits were closed after the passage of the wave packet to avoid reflection from the boundary of the grid, see (5); $t_c = 0.5$, $\gamma = 4$.)

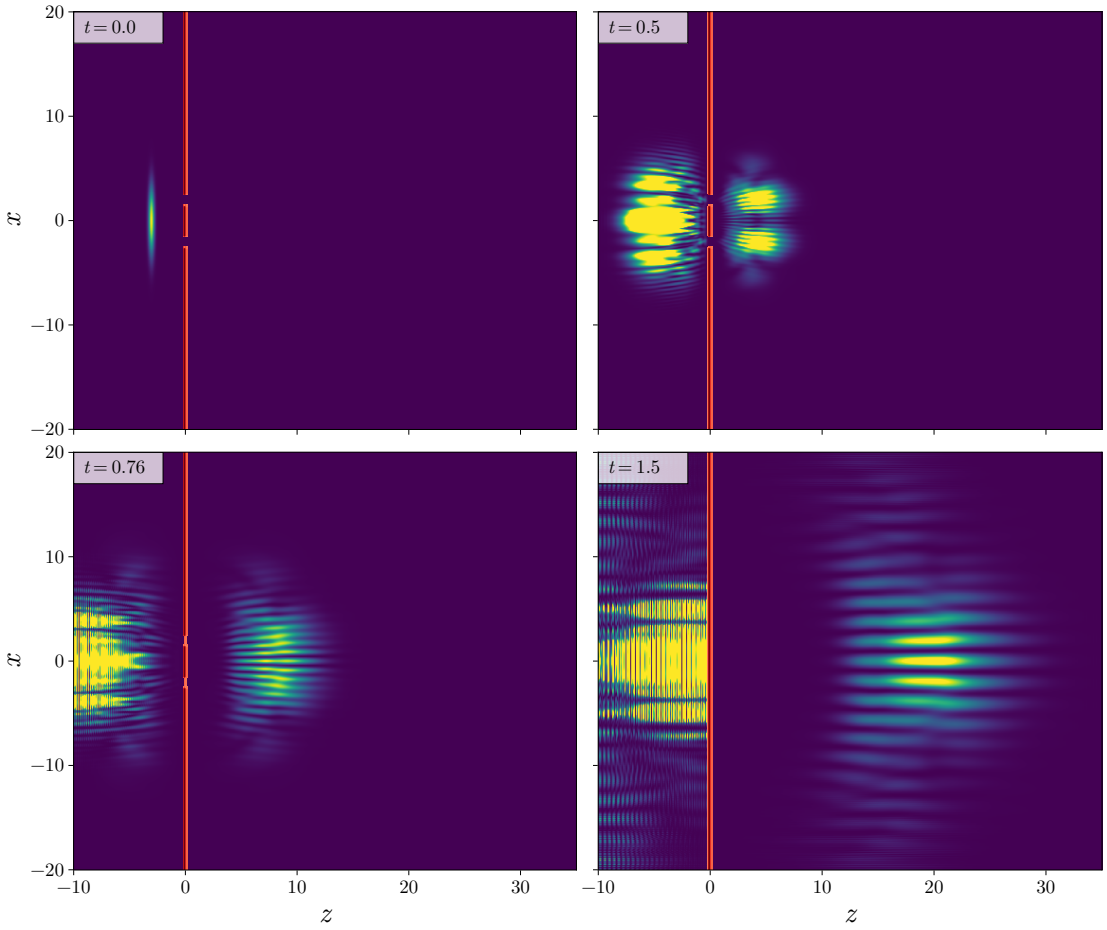

Figure 4: A few snapshots of the evolving $|\psi|^2$-density, using the same parameters as in Fig. 3a. Note the closing of the slits (see (5); $t_c = 0.75$, $\gamma = 4$) to prevent the reflected wave from influencing the arrivals.

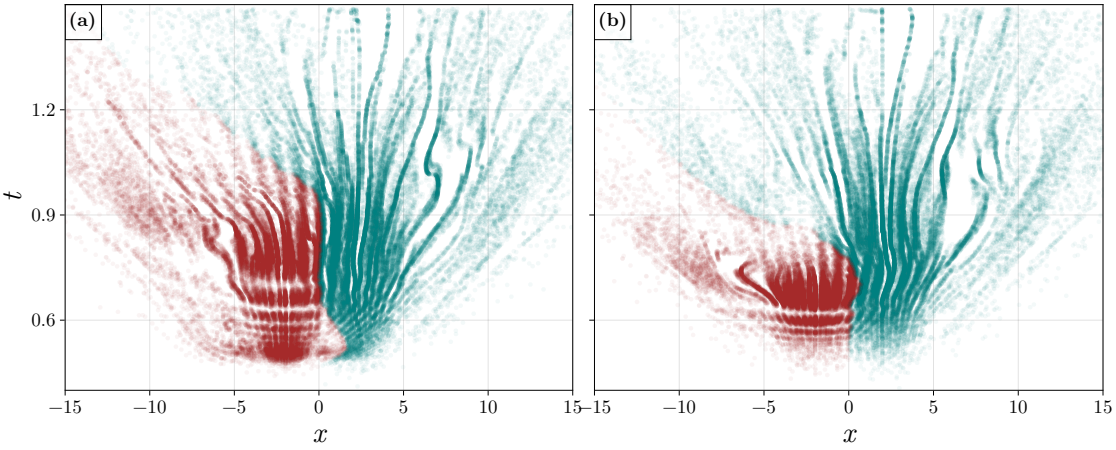

Figure 5: Scatter plot of $\approx 10^5$ Bohmian trajectories arriving at $d = 10$ over time for the dynamic DSE, where the slit centered at $x = -\Delta$ ($= -1$ in our units) is closed in flight around time $t_c = 0.25$: **(a)** Fast closing $\gamma = 100$, **(b)** Slow closing $\gamma = 20$. Data points for trajectories passing through the closing (open) slit are rendered in brown (cyan). The potential barrier and initial wave packet parameters are same as for Fig. 3a.

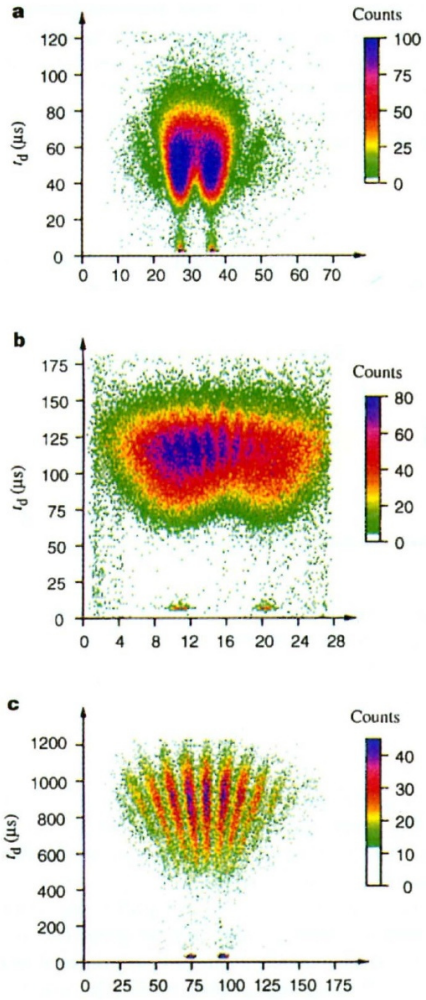

Figure 6: Experimental data for He* atoms with $d = 148\,\text{mm}$ (a), $d = 248\,\text{mm}$ (b), and $d = 1,950\,\text{mm}$ (c) (reproduced from [10] with permission). Here, $t_d = (d/L)\,t_f$ is a "scaled time-of-flight", where L is the source-to-screen separation.

3 Comparison to the KPM experiment

As mentioned in the introduction, there have been many realizations of the double-slit experiment. An experiment of particular interest is that of KPM [10], which recorded not only the detected positions, but also the flight times. The resulting joint position and time distribution is shown in Fig. 6, for three different locations of the detection screen. These experimentally obtained distributions show qualitative similarity to the Bohmian distributions shown in Fig. 3a. However, this similarity is deceiving.

Let us first consider the details of the KPM experiment. In the experiment, metastable helium atoms (denoted He*) are sourced from a gas-discharge tube by firing a $15\,\mu$s pulse of electric current. Some spurious fast-moving atoms along with slower atoms with velocities ranging between $1 - 3 \times 10^3\,\text{ms}^{-1}$ are produced by the source. The ejected atoms pass through a skimmer and are collimated by a $5\,\mu$m-wide slit. Further downstream, they encounter a microfabricated double-slit structure of slit separation $2\Delta = 8\,\mu$m and slit-width $\sigma_s = 1\,\mu$m, eventually striking the detector plate at d. He* atoms eject secondary electrons upon hitting the conductive surface of the detector—a process assumed to take place on a time scale of $10^{-12}\,$s. These electrons are

carefully imaged onto a single-electron detection unit based on a chevron assembly of multichannel plates [53]. The spatial (temporal) resolution achieved with this detector is of the order of 500 nm (100 ns). For three different slit-screen separations d, KPM recorded the detection events (x, y, t_f) of individual atoms by repeatedly firing the source, shown in Fig. 6. Notice that the fast atoms produce a "geometrical shadow" of the slits at the bottom of each figure [10, p. 151]. In the KPM experiment, the ToF from the source to the detection is rescaled as $t_d = (d/L)t_f$, with L the source-to-screen separation, taken to be the time from the passage through the slits to the screen.

While the KPM plots show a striking similarity with the Bohmian plots, there is an important difference. We have employed *the same initial wave function* for each run of the DSE, whereas the discharge tube in the KPM experiment yields a *statistical mixture of wave packets* of different longitudinal velocities, thermally distributed, see [54, Fig. 4]. The mixed state character together with the fact that the longitudinal velocities are a few thousand meters per second implies that the temporal spread of the distributions plotted in Fig. 6 stems mainly from the spread of the velocity distribution and *not* from the longitudinal spread of the initial packet. This is also why KPM treat the longitudinal motion classically. (And why it makes sense to consider the rescaled time $t_d = (d/L)t_f$ to represent the time between detection and passage through the screen.) This is unlike our Bohmian simulations, where the temporal spread in the distribution stems solely from the longitudinal spread of the wave packet.

Let us back up these statements quantitatively. For this, assume that, on the contrary, the temporal spread is largely due to the longitudinal spread of the wave packets and that the mixed state character (which is unavoidable) only plays a minor role. Consider for example the parameters for Fig. 6 (c). The temporal spread in this figure is several hundreds of μs. Let us assume therefore that a single wave packet can produce a spread in the detection time of at least, say, 100μs. Taking a velocity of $10^3 \mathrm{ms}^{-1}$, this means that the longitudinal width of the wave packet is of the order of $10^5 \mu$m. (This is assuming that detections take place while the bulk of the wave packet crosses the detection screen.) Assuming Gaussian spreading so that the width $\sigma(t)$ at time t is given by $\sigma(t) = \sigma\sqrt{1 + (\hbar t/m\sigma^2)^2}$, with σ the initial width, $m = 6.64 \times 10^{-27}$kg the mass of a Helium atom, and taking t to be the time to traverse 3m, which is the distance between the collimating slit and the detection screen (see [10, Fig. 2]), with a velocity of $10^3 \mathrm{ms}^{-1}$, we find that a final width of $\sigma(t) = 10^5 \mu$m implies an initial width $\sigma \approx 5 \times 10^{-4} \mu$m. This is much smaller than the transverse dimensions of the setup, like the transverse width of 5μm of the collimating slit or the distance between the slits of 8μm. Conversely, assume a longitudinal width of a wave function of 5μm at the time of passage through the collimating slit (so the same as the transverse width of this slit). Assuming again Gaussian spreading, the width will be less than 10μm by the time the wave function crosses the screen. This will entail a temporal spread of merely $10^{-2} \mu$s, which is even smaller than the detector resolution of $10^{-1} \mu$s.

It is also the case that the temporal spread displayed in the figure can be accounted for by the spread of the velocities. With velocities ranging from 10^3m to 3×10^3m, the associated temporal spread is of the order of $10^3 \mu$m, which agrees with what is shown in Fig. 6 (c).

In conclusion, in the KPM experiment the ToF is determined by the time each wave packet crosses the detection screen and does not require a quantum treatment (even though this could of course be covered using the Bohmian dynamics). The same holds for other experimental realizations to date. To explore the quantum aspect of the ToF in the case of the double-slit experiment, the wave packet should have a ratio of longitudinal spread and velocity that is much larger than the temporal detector resolution. In addition, the initial velocity should be controlled as precisely as possible to reduce velocity spread. Ultracold neutrons which have a velocity of about 1m/s may be a possibility [14]. Alternatively, one could perhaps consider a different placement of the detection screen, as recently proposed in [77].

4 Concluding remarks

The computation of the probability distribution of ToFs of quantum particles is one of the last areas where experts disagree about what quantum mechanics should predict. While a cornucopia of different ToF distributions exists in the literature, one rarely finds a discussion of the joint distribution of impact positions *and* ToFs studied in this work. In this paper, we have considered a Bohmian approach to this problem.

While the KPM experiment reported a joint position and time distribution, it is not suitable to test quantum aspects of ToF proposals. However, DSE setups do have the potential to do this. To make progress with this question, we recommend that ToF-resolved DSEs and dynamic variants thereof, as described in this work, should be performed with present-day technology to achieve a *quantitative* experiment-to-theory comparison in the future. A particular improvement would be better control of the initial wave packet of the particle, e.g., sourcing the particle from an ion trap post-cooling [79], or using field-emission-tip electron wave packets à la [80], both of which offer better initial wave packet control compared to a gas-discharge source.

Acknowledgements. J. Dziewior, C. Kurtsiefer, T. Maudlin, M. Mukherjee, S. Goldstein, R. Tumulka, N. Zanghì, and H. Ulbricht are thanked for fruitful discussions, H. Weinfurter for suggesting the dynamic DSE, J. M. Wilkes for editorial inputs, and the referees for valuable comments. L.K. and D.-A.D. acknowledge funding from the Elite Network of Bavaria, through the Junior Research Group "Interaction Between Light and Matter". W.S. is supported by the Research Foundation Flanders (Fonds Wetenschappelijk Onderzoek, FWO), Grant No. G0C3322N. We dedicate this work to the memory of Detlef Dürr.

References

[1] R. Feynman, R. Leighton, and M. Sands, *The Feynman Lectures on Physics, Quantum Mechanics Vol. III* (Basic Books, 2011).

[2] W. K. Wootters and W. H. Zurek, "Complementarity in the double-slit experiment: Quantum nonseparability and a quantitative statement of Bohr's principle", Phys. Rev. D **19**, 473–484 (1979).

[3] S. M. Tan and D. F. Walls, "Loss of coherence in interferometry", Phys. Rev. A **47**, 4663–4676 (1993).

[4] J. A. Wheeler, "The "Past" and the "Delayed-Choice" Double-Slit Experiment", in *Mathematical foundations of quantum theory*, edited by A. Marlow (Academic Press, 1978), pp. 9–48.

[5] R. Bach, D. Pope, S.-H. Liou, and H. Batelaan, "Controlled double-slit electron diffraction", New J. Phys. **15**, 033018 (2013).

[6] A. Tonomura, J. Endo, T. Matsuda, T. Kawasaki, and H. Ezawa, "Demonstration of single-electron buildup of an interference pattern", Am. J. Phys. **57**, 117–120 (1989).

[7] A. Zeilinger, R. Gähler, C. G. Shull, W. Treimer, and W. Mampe, "Single- and double-slit diffraction of neutrons", Rev. Mod. Phys. **60**, 1067–1073 (1988).

[8] R. Gähler and A. Zeilinger, "Wave-optical experiments with very cold neutrons", Am. J. Phys. **59**, 316–324 (1991).

[9] O. Carnal and J. Mlynek, "Young's double-slit experiment with atoms: A simple atom interferometer", Phys. Rev. Lett. **66**, 2689–2692 (1991).

[10] C. Kurtsiefer, T. Pfau, and J. Mlynek, "Measurement of the Wigner function of an ensemble of helium atoms", Nature **386**, 150–153 (1997).

[11] C. Brand, S. Troyer, C. Knobloch, O. Cheshnovsky, and M. Arndt, "Single-, double-, and triple-slit diffraction of molecular matter waves", Am. J. Phys. **89**, 1132–1138 (2021).

[12] R. Werner, "Screen observables in relativistic and nonrelativistic quantum mechanics", J. Math. Phys. **27**, 793–803 (1986).

[13] M. Daumer, D. Dürr, S. Goldstein, and N. Zanghì, "On the Quantum Probability Flux Through Surfaces", J. Stat. Phys. **88**, 967–977 (1997).

[14] A. Viale, Vicari, M., and N. Zanghì, "Analysis of the loss of coherence in interferometry with macromolecules", Phys. Rev. A **68** (2003).

[15] D. Dürr and S. Teufel, *Bohmian Mechanics: The Physics and Mathematics of Quantum Theory* (Springer-Verlag, Berlin, 2009).

[16] J. G. Muga and C. R. Leavens, "Arrival time in quantum mechanics", Phys. Rep. **338**, 353–438 (2000).

[17] J. Muga, R. Sala, and J. Palao, "The time of arrival concept in quantum mechanics", Superlattices Microstruct. **23**, 833–842 (1998).

[18] S. Das and D. Dürr, *Benchmarking quantum arrival time distributions using a back-wall*, in preparation.

[19] B. Mielnik and G. Torres-Vega, "Time Operator: the challenge persists", Concepts of Physics **II**, 81–97 (2005).

[20] C. R. Leavens, "On the "standard" quantum mechanical approach to times of arrival", Phys. Lett. A **303**, 154–165 (2002).

[21] I. Egusquiza, J. Muga, B. Navarro, and A. Ruschhaupt, "Comment on: "On the standard quantum-mechanical approach to times of arrival", Phys. Lett. A **313**, 498–501 (2003).

[22] C. R. Leavens, "Reply to Comment on: "On the 'standard' quantum-mechanical approach to times of arrival" [Phys. Lett. A 313 (2003) 498]", Phys. Lett. A **345**, 251–257 (2005).

[23] S. Das and M. Nöth, "Times of arrival and gauge invariance", Proc. R. Soc. A. **477**, 20210101 (2021).

[24] S. Das and W. Struyve, "Questioning the adequacy of certain quantum arrival-time distributions", Phys. Rev. A **104**, 042214 (2021).

[25] W. Cavendish, S. Das, M. Nöth, and A. A. Rafsanjani, *(Un)physical consequences of "Quantum Measurements of Time"*, 2024.

[26] C. Spielmann, R. Szipöcs, A. Stingl, and F. Krausz, "Tunneling of Optical Pulses through Photonic Band Gaps", Phys. Rev. Lett. **73**, 2308–2311 (1994).

[27] A. M. Steinberg, P. G. Kwiat, and R. Y. Chiao, "Measurement of the single-photon tunneling time", Phys. Rev. Lett. **71**, 708–711 (1993).

[28] T. Zimmermann, S. Mishra, B. R. Doran, D. F. Gordon, and A. S. Landsman, "Tunneling Time and Weak Measurement in Strong Field Ionization", Phys. Rev. Lett. **116**, 233603 (2016).

[29] U. S. Sainadh, R. T. Sang, and I. V. Litvinyuk, "Attoclock and the quest for tunnelling time in strong-field physics", J. Phys. Photonics **2**, 042002 (2020).

[30] R. Ramos, D. Spierings, I. Racicot, and A. M. Steinberg, "Measurement of the time spent by a tunnelling atom within the barrier region", Nature **583**, 529–532 (2020).

[31] C. Leavens, "Time of arrival in quantum and Bohmian mechanics", Phys. Rev. A **58**, 840–847 (1998).

[32] C. R. Leavens, "Timing quantum particles from the perspective of Bohmian mechanics", Superlattices Microst. **23**, 795–807 (1998).

[33] G. Grübl and K. Rheinberger, "Time of arrival from Bohmian flow", J. Phys. A: Math. Gen. **35**, 2907–2924 (2002).

[34] J. T. Cushing, "Quantum tunneling times: a crucial test for the causal program?", Found. Phys. **25**, 269–280 (1995).

[35] M. Kazemi and V. Hosseinzadeh, "On detection statistics in double-double-slit experiment", arXiv:2208.01325 (2022).

[36] W. Xie, M. Li, Y. Zhou, and P. Lu, "Interpreting attoclock experiments from the perspective of Bohmian trajectories", Phys. Rev. A **105**, 013119 (2022).

[37] C. R. Leavens, "The "Tunneling-Time Problem" for Electrons", in *Bohmian Mechanics and Quantum Theory: An Appraisal*, edited by J. T. Cushing, A. Fine, and S. Goldstein (Springer Netherlands, Dordrecht, 1996), pp. 111–129.

[38] C. Leavens, "Arrival time distributions", Phys. Lett. A **178**, 27–32 (1993).

[39] N. Douguet and K. Bartschat, "Dynamics of tunneling ionization using Bohmian mechanics", Phys. Rev. A **97**, 013402 (2018).

[40] S. Das and D. Dürr, "Arrival Time Distributions of Spin-1/2 Particles", Sci. Rep. **9**, 2242 (2019).

[41] S. Das, M. Nöth, and D. Dürr, "Exotic Bohmian arrival times of spin-1/2 particles: An analytical treatment", Phys. Rev. A **99**, 052124 (2019).

[42] X. Oriols, F. Martín, and J. Suñé, "Implications of the noncrossing property of Bohm trajectories in one-dimensional tunneling configurations", Phys. Rev. A **54**, 2594–2604 (1996).

[43] S. V. Mousavi and M. Golshani, "Causal description of the interaction of a two-level atom with a classical field", Phys. Scr. **78**, 035007 (2008).

[44] S. V. Mousavi, "Scattering by a reflectionless modified Pöschl–Teller potential: Bohmian trajectories and arrival times", Phys. Scr. **90**, 095001 (2015).

[45] Y. Nogami, F. Toyama, and W. van Dijk, "Bohmian description of a decaying quantum system", Phys. Lett. A **270**, 279–287 (2000).

[46] M. Ruggenthaler, G. Grübl, and S. Kreidl, "Times of arrival: Bohm beats Kijowski", J. Phys. A: Math. Gen. **38**, 8445–8451 (2005).

[47] A. K. Pan and D. Home, "On Empirical Scrutiny of the Bohmian Model Using a Spin Rotator and the Arrival/Transit Time Distribution", Int. J. Theor. Phys **51**, 374–389 (2012).

[48] D. Home and A. S. Majumdar, "On the Importance of the Bohmian Approach for Interpreting CP-Violation Experiments", Found. Phys. **29**, 721–727 (1999).

[49] A. S. Majumdar and D. Home, "Interpreting the measurement of time of decay: phenomenological significance of the Bohm model", Phys. Lett. A **296**, 176–180 (2002).

[50] S. V. Mousavi and M. Golshani, "Bohmian approach to spin-dependent time of arrival for particles in a uniform field and for particles passing through a barrier", J. Phys. A: Math. Theor. **41**, 375304 (2008).

[51] D. Demir, "Scattering times of quantum particles from the gravitational potential and equivalence principle violation", Phys. Rev. A **106**, 022215 (2022).

[52] G. E. Field, "On the status of quantum tunnelling time", Euro. Jnl. Phil. Sci. **12** (2022).

[53] C. Kurtsiefer and J. Mlynek, "A 2-dimensional detector with high spatial and temporal resolution for metastable rare gas atoms", Appl. Phys. B **64**, 85–90 (1996).

[54] T. Pfau and C. Kurtsiefer, "Partial reconstruction of the motional Wigner function of an ensemble of helium atoms", J. Mod. Opt. **44**, 2551–2564 (1997).

[55] D. Bohm and B. J. Hiley, *The Undivided Universe: An Ontological Interpretation of Quantum Theory* (Routledge, London and New York, 1993).

[56] P. R. Holland, *The quantum theory of motion: an account of the de Broglie-Bohm causal interpretation of quantum mechanics* (Cambridge university press, 1995).

[57] D. Dürr, S. Goldstein, and N. Zanghì, "Quantum Equilibrium and the Role of Operators as Observables in Quantum Theory", J. Stat. Phys. **116**, 959–1055 (2004).

[58] C. Philippidis, C. Dewdney, and B. Hiley, "Quantum interference and the quantum potential", IL Nuov Cim B **52**, 15–28 (1979).

[59] C. Philippidis, D. Bohm, and R. D. Kaye, "The Aharonov-Bohm effect and the quantum potential", IL Nuov Cim B **71**, 75–88 (1982).

[60] A. S. Sanz, F. Borondo, and S. Miret-Artés, "Particle diffraction studied using quantum trajectories", J. Phys.: Condens. Matter **14**, 6109–6145 (2002).

[61] P. Holland and C. Philippidis, "Implications of Lorentz covariance for the guidance equation in two-slit quantum interference", Phys. Rev. A **67**, 062105 (2003).

[62] M. Gondran and A. Gondran, "Numerical simulation of the double slit interference with ultracold atoms", Am. J. Phys. **73**, 507–515 (2005).

[63] S. Kocsis et al., "Observing the Average Trajectories of Single Photons in a Two-Slit Interferometer", Science **332**, 1170–1173 (2011).

[64] J. S. Bell, *Speakable and Unspeakable in Quantum Mechanics: Collected Papers on Quantum Philosophy* (Cambridge University Press, 2004).

[65] L. D. Landau and E. M. Lifshitz, *Quantum Mechanics: Nonrelativistic theory*, third, Vol. 3, Course of Theoretical Physics (Pergamon Press, Moscow, 1977).

[66] S. Kreidl, G. Grübl, and H. G. Embacher, "Bohmian arrival time without trajectories", J. Phys. A: Math. Gen. **36**, 8851–8865 (2003).

[67] M. Daumer, D. Dürr, S. Goldstein, and N. Zanghì, "On the flux-across-surfaces theorem", Lett. Math. Phys. **38**, 103–116 (1996).

[68] N. Vona, G. Hinrichs, and D. Dürr, "What Does One Measure When One Measures the Arrival Time of a Quantum Particle?", Phys. Rev. Lett. **111**, 220404 (2013).

[69] S. Goldstein, R. Tumulka, and N. Zanghì, "Arrival Times Versus Detection Times", Found. Phys. **54** (2024).

[70] S. Das and S. Aristarhov, *Comment on "the Spin Dependence of Detection Times and the Nonmeasurability of Arrival Times"*, 2023.

[71] R. Tumulka, *Foundations of Quantum Mechanics*, Lecture Notes in Physics (Springer International Publishing, 2022).

[72] E. Nelson, "Derivation of the Schrödinger Equation from Newtonian Mechanics", Phys. Rev. **150**, 1079–1085 (1966).

[73] S. Colin and H. Wiseman, "The Zig-Zag Road to Reality", J. Phys. A: Math. Theor. **44**, 345304 (2011).

[74] W. Struyve, "On the Zig-Zag Pilot-Wave Approach for Fermions", J. Phys. A: Math. Theor. **45**, 195307 (2012).

[75] H. Nitta and T. Kudo, "Time of arrival of electrons in the double-slit experiment", Phys. Rev. A **77**, 014102 (2008).

[76] C. Maes, K. Meerts, and W. Struyve, "Diffraction and interference with run-and-tumble particles", Physica A, 127323 (2022).

[77] A. Ayatollah Rafsanjani, M. Kazemi, A. Bahrampour, and M. Golshani, "Can the double-slit experiment distinguish between quantum interpretations?", Communications Physics **6** (2023).

[78] S. Krekels, *DSE Arrival Times*, `https://gitlab.kuleuven.be/u0133590/dse-arrival-times`, 2024.

[79] F. Stopp, H. Lehec, and F. Schmidt-Kaler, "A deterministic single ion fountain", Quantum Sci. Technol. (2022).

[80] E. Jones, M. Becker, J. Luiten, and H. Batelaan, "Laser control of electron matter waves", Laser Photon Rev. **10**, 214–229 (2016).